A novel mechanism for host-mediated photoprotection in endosymbiotic foraminifera

Katherina Petrou*[1], Peter J. Ralph[2] & Daniel A. Nielsen[1]

[1]School of Life Sciences, University of Technology Sydney, PO Box 123, Broadway, New South Wales, 2007, Australia.

[2]Climate Change Cluster, University of Technology Sydney, PO Box 123, Broadway, New South Wales, 2007, Australia.

*Corresponding author:

Dr Katherina Petrou

katherina.petrou@uts.edu.au

Phone: +61 2 9514 4159

Key words: symbiosis, foraminifera, *Marginopora vertebralis*, photoprotection, *Symbiodinium*

Abstract

Light underpins the health and function of coral reef ecosystems, where symbiotic partnerships with photosynthetic algae constitute the life support system of the reef. Decades of research have given us detailed knowledge of the photo-protective capacity of phototrophic organisms, yet little is known about the role of the host in providing photoprotection in symbiotic systems. Here we show that the intracellular symbionts within the large photo-symbiotic foraminifera *Marginorpora vertebralis* exhibit phototactic behaviour, and that the phototactic movement of the symbionts is accomplished by the host, through rapid actin-mediated relocation of the symbionts deeper into the cavities within the calcium carbonate test. Using a photosynthetic inhibitor, we identified that the info-chemical signalling for host regulation is photosynthetically derived, highlighting the presence of an intimate communication between the symbiont and the host. Our results emphasise the central importance of the host in photo-symbiotic photoprotection via a new mechanism in foraminifera that can serve as a platform for exploring host-symbiont communication in other photo-symbiotic organisms.

Introduction

The benthic foraminifera *Marginopora vertebralis* (Quoy & Gaimard, 1830) is a large, single-celled, calcifying micro-organism belonging to the infrakingdom *Rhizaria*. It is typically found in coral reef ecosystems, where it is a major contributor to calcite export from the surface waters to the reef structure, with calcium carbonate tests (calcite skeletons) often dominating the sediment (Langer et al, 1997; Doo et al, 2012). *M. vertebralis* forms a symbiotic partnership with one of the most important symbiotic algal species in tropical reef systems, the dinoflagellate *Symbiodinium* (Pawlowski et al, 2001), renowned for living in endosymbioses with reef-building corals across the globe (Baker, 2003). This partnership has evolved to make use of the abundance of light in the clear, nutrient-poor waters of the reef; whereby the host receives energy from the photosynthetic symbiont in the form of fixed carbon (Lee, 2006) in exchange for providing the symbiont with access to a rich supply of inorganic nutrients. While light underpins the health and function of coral reef ecosystems, in excess, light can results in reduced photosynthetic efficiency, and if not protected against, damage to the photosynthetic machinery of the symbiont can ensue (Brown et al, 1999; Jones and Hoegh-Guldberg, 2001). Therefore, the success of photo-symbiotic partnerships relies on the ability for the symbiont and host to regulate incoming irradiance with nutrient acquisition, serving two purposes: 1) to optimise carbon productivity by the symbionts, ultimately benefitting the host, and 2) to minimise the production of reactive oxygen species which may damage both symbiont and host.

The ubiquity of *Symbiodinium* in reef symbioses has resulted in extensive research into understanding light regulation and stress responses in these microalgae (Iglesias-Prieto and Trench, 1994; Iglesias-Prieto and Trench, 1997; Jones and Hoegh-Guldberg, 2001). In corals – the most extensively studied photosymbiotic system in tropical reefs – photoprotection is primarily regulated by the *Symbiodinium*, which have evolved mechanisms to dissipate excess energy as heat and thus protect their photosystems from damage (Brown et al, 1999). It has also been shown that the coral host can contribute to light protection via accumulation of fluorescent proteins that absorb light in

61 the harmful wavelengths (Salih et al, 2000; Dove et al, 2008), or more directly via contraction or
62 expansion of tissue, which modulates the light field around the symbionts within specific tissue
63 layers (Brown et al, 2002; Dimond et al, 2012; Wangpraseurt et al, 2014). Similar to corals, *M.*
64 *vertebralis* is often found in shallow, well-lit waters of the sandy reef sediment (Sinutok et al, 2011),
65 and therefore must balance incoming energy with photoprotection. Unlike corals however, *M.*
66 *vertebralis* are motile and as such can achieve photoprotection through relocation to more shaded
67 habitats. Indeed, *M. vertebralis* has been shown to exhibit negative phototaxis; moving into a shaded
68 environment when exposed to high light, a response proposed to be driven by the light sensitive
69 symbionts (Sinutok et al, 2013). Their movement is, however, relatively slow (up to 8 mm h^{-1})
70 (Khare and Nigam, 2000) and thus ineffective in providing immediate protection from damaging
71 irradiances once exposed. One study has reported a different sort of phototaxis in stationary *M.*
72 *vertebralis*, where the symbionts were observed to move vertically within the calcified test from the
73 darker underside to the illuminated top-side (Ross, 1972). While not examined in any detail, this
74 movement was assumed to be the result of flagellated *Symbiodinium* swimming towards the light
75 inside the host test. Here we investigate whether intracellular phototaxis could be used as a means of
76 photoprotection. We show that vertical migration of symbionts within *M. vertebralis* serves to
77 rapidly and effectively protect the intracellular symbionts under high light stress. This mode of
78 symbiont migration represents a novel mechanism in which the phototaxis of the symbionts is host-
79 mediated; the relocation of the symbionts being accomplished through host-derived actin filament
80 contraction as opposed to driven by flagellated movement of the symbionts, as was previously
81 assumed. Our study reveals a novel regulatory mechanism for host-mediated photoprotection that
82 may serve as a platform for studying host-symbiont communication in other photo-symbiotic
83 organisms such as corals, providing a new means for investigating signalling between the ubiquitous
84 *Symbiodinium* algae and its host.

85

Materials and Methods

Sample collection and experimental design: Individual specimens of *Marginopora vertebralis* were collected from the inner reef flat of Heron Island, Great Barrier Reef, Australia (July 2014) and maintained at 22°C in aquaria with flow-through artificial seawater on a 12:12 h (light:dark) cycle for several weeks prior to the experiment. Light was supplied from a programmable blue/white LED panel (2-channel Phantom, CIDLY Ltd, Shenzhen, China) providing a coarse sinusoidal light cycle (16-step light levels) with a midday maximum of 130 µmol photons m^{-2} s^{-1}. To investigate intracellular phototaxis in *M. vertebralis*, foraminifera were transferred into small beakers with 100 mL of artificial seawater and placed into two temperature-controlled water baths (maintained at 22 °C) and left for 1 h prior to initial measurements (T0). The light treatment consisted of incremental increases every hour (from 130 to 200, 400 and 800 µmol photons m^{-2} s^{-1}), followed by a recovery period at 130 µmol photons m^{-2} s^{-1}. Control incubations were kept at 130 µmol photons m^{-2} s^{-1} throughout the experiment. Light levels were selected based on the mean minimum saturating irradiance (108 ± 4 µmol photons m^{-2} s^{-1}) and photoinhibiting irradiance (301 ± 12 µmol photons m^{-2} s^{-1}) determined from steady state light curves (rETR vs PAR) performed on individuals of *M. vertebralis* (n=6) prior to the experiment (see Supplementary Figure S1). The experiment was repeated using 5 µg mL^{-1} of the actin filament inhibitor cytochalasin B (n=5-8) and to investigate the effect of 10 µM DCMU (n=6-8). In both cases DMSO was added to the controls at the same concentration (0.1% v/v). At each time point (T0-T4), chlorophyll *a* fluorescence, colour change and reflectance were measured (see below) and individuals were sampled for pigment analyses and histological sectioning.

Symbiont photosystem activity and photoprotective pigments: Photosynthetic efficiency of the algal symbionts was measured on the surface and underside of the foraminifera (n=8) via chlorophyll

110 *a* fluorescence using a Pulse Amplitude Modulated (PAM) fluorometer (Imaging-PAM, MAXI
111 version, Walz GmbH, Effeltrich, Germany). At each time point, the beaker containing the
112 foraminifera was transferred to the PAM and a saturating pulse of light (saturating pulse width = 0.8
113 s; saturating pulse intensity > 3000 μmol photons m^{-2} s^{-1}) applied to determine minimum (F_O') and
114 maximum fluorescence (F_M'). Individuals were then carefully flipped using forceps and the underside
115 measured before being returned to their original orientation and placed back into the incubation bath.
116 From these two parameters the effective quantum yield of PSII was calculated as $\Delta F/F_M' = (F_M' -$
117 $F_O')/ F_M'$ (Schreiber 2004). Additionally, prior to the experiment, foraminifera were dark-adapted for
118 30min and F_O and F_M recorded to calculate F_V/F_M as $(F_M - F_O)/ F_M$ (Schreiber 2004). This was
119 repeated at the end of the experiment in both control and light treated foraminifera, to measure
120 recovered F_V/F_M. As a measure of photosynthetic performance at each specific irradiance, excitation
121 pressure over PSII (Q_M) was calculated as 1- ($\Delta F/F_M' / F_V/F_M$) (Iglesias-Prieto et al., 2004). As there
122 was minimal spatial variability in fluorescence signal, all fluorescence values were therefore
123 averaged across the organism. At each time point, 3 individuals from both light treatments were snap
124 frozen in liquid nitrogen and stored at -80°C for pigment processing. Individual foraminifera were
125 extracted in chilled 100% acetone containing vitamin E and sonicated for 30 min in iced-water in the
126 dark, then stored in the dark at 4 °C. After 24h, 333 μL of polished water was added to reduce the
127 acetone concentration to 90% v/v and sonicated for 15 min in iced-water. The foraminifer test was
128 then removed and dried for area determination (see below). The acetone extracts were filtered
129 directly into amber glass vials (Waters Australia Pty Ltd, Rydalmere, Australia) through a 0.2 μm
130 PTFE 13 mm syringe filter (Micro-Analytix Pty Ltd, Taren Point, NSW, Australia) pre-wetted with
131 acetone, and stored at -80 °C until analysis via high performance liquid chromatography (HPLC)
132 following the methods of van Heukelem and Thomas (2001). Pigments were identified by
133 comparison of their retention times and spectra using calibration standards (DHI, Hørsholm,
134 Denmark) and integrated using graphical software (Empower Pro, Waters Australia Pty Ltd,

135 Rydalmere, NSW, Australia). For area determination, each test was imaged and measured in ImageJ
136 (Schneider et al. 2012), using the area integration function calibrated to a known standard.

137

138 **Foraminifer colour change:** Individuals were imaged with a digital microscope colour camera
139 (MU500, Amscope, Irvine, USA) attached to a dissection microscope (SM-6TY, Amscope, Irvine,
140 USA). The colour intensity of each foraminifer was measured with ImageJ software (Schneider et
141 al., 2012) by integrating the pixel intensity (whiteness) of the whole foraminifer. Pixel intensity was
142 processed relative to the initial pixel intensity of each individual and only foraminifera with a
143 uniform distribution of symbionts over their entire surface were included in the final data (minimum
144 $n = 5$).

145

146 **Surface reflectance:** Surface reflectance was measured using a polished glass fibre (Ocean Optics
147 inc., Dunedin, USA) connected to a spectrophotometer (USB2000, Ocean Optics inc., Dunedin,
148 USA) using dedicated software (SpectraSuite, Ocean Optics inc., Dunedin, USA). The glass fibre
149 was positioned at a fixed distance and angle (45°) from the foraminifera surface using a manual
150 micromanipulator (Unisense, Aarhus, Denmark). Reflectance was recorded for each individual (n=8)
151 and the resultant spectra were standardised against absolute reflectance (white diffuse reflectance
152 standard, Spectralon® SRS-99, LabSphere inc., North Sutton, United Kingdom).

153

154 **Histology:** Foraminifera were fixed in 1 mL 2.5% glutaraldehyde in phosphate buffered saline (1X
155 PBS; NaCl: 8.0, KCl: 0.2, Na_2HPO_4: 1.44, KH_2PO_4: 0.25 g L^{-1}) for 24 h at 4 °C and then washed
156 twice with 1X PBS. Decalcification was carried out overnight in 10% w/w EDTA (pH 8.0) after
157 which the remaining tissue was washed to remove residual EDTA. All solutions contained 0.65 mol

158 L^{-1} sucrose to ensure minimal osmotic stress. Tissue from decalcified foraminifera was embedded in
159 paraffin wax using an enclosed automated tissue processor (Shandon Excelsior ES®, Thermo Fisher
160 Scientific inc., Waltham, USA) and a standard ethanol and xylen dehydration method. The
161 embedded foraminifera were cut into 15 µm sections using a microtome and dried onto hydrophilic
162 slides (StarFrost, Waldemar Knittel, Braunschweig, Germany). Tissue sections were visualised on an
163 inverted fluorescence microscope (Eclipse-T*i*, Nikon Corporation, Japan) using the auto-
164 fluorescence of the animal tissue (FITC, blue/green ex 475-490 nm/em 500-540 nm) and symbiont
165 chlorophyll (TexasRed, green/red ex 532-587 nm/em 595 nm).

166

167 **Video analysis of symbiont movement:** Using an inverted fluorescence microscope symbionts were
168 imaged inside the chambers of live foraminifera in the presence and absence of cytochalasin B
169 (n=18). Chambers of the foraminifera were imaged in two fluorescent wavelengths (Green – FITC,
170 red – TexasRed) at a total of 400X magnification, utilising the auto-fluorescence of the skeleton and
171 symbionts, respectively. Foraminifera were left in the dark and an image taken every minute for 15
172 minutes. For analyses, only chambers which were less than half full of symbionts were included to
173 avoid bias resulting from clumping of cells, and only cells visible for the full length of the image
174 series were included in the analyses. The movement of individual symbionts was measured by
175 calculating the change in location of each symbiont between images.

176

177 **Statistical analysis:** Chlorophyll *a* fluorescence and relative change in pixel intensity as a function
178 of time were analysed using repeated measures analysis of variance (rmANOVA) for the interactive
179 terms of treatment and time (α = 0.05). Differences in photoprotective pigments, symbiont
180 movement in the presence and absence of cytochalasin B, as well as the relative change in
181 reflectance and effective quantum yield of PSII in the presence and absence of DCMU were analysed

using one-way ANOVA ($\alpha = 0.05$). All data were checked *a priori* for normality and homoscedasticity. In the cases where data failed to meet the assumptions, data were transformed. All data were analysed using statistical software package SPSS (v.22; IBM, Armonk, New York, USA).

Results

Symbionts exhibit negative phototaxis under photosynthetic stress

Exposure to incremental increases in irradiance resulted in a significant decline ($P = 0.001$) in the effective quantum yield of PSII ($\Delta F/F_M'$). The $\Delta F/F_M'$ dropped to 0.1 when exposed to 800 µmol photons m^{-2} s^{-1} for 1 h (Figure 1a). The recovery of $\Delta F/F_M'$ in the foraminifera exposed to the high light treatment reached 75% of the initial $\Delta F/F_M'$ while there was no change in $\Delta F/F_M'$ in the foraminifera maintained at 130 µmol photons m^{-2} s^{-1} (Figure 1a). In both of the light treatments, the underside of *M. vertebralis* showed significantly higher ($P < 0.001$) quantum yield values (0.590; dark-adapted) and no change over time (Figure 1a), suggesting the cells located on the underside of the test were completely protected from the high irradiances. Excitation pressure over PSII (Q_M), a measure of the proportion of open PSII reaction centres, increased significantly with increasing irradiance ($P < 0.001$), reaching a maximum value of 0.83 at the highest irradiance (Figure 1b). Consistent with the recovery in $\Delta F/F_M'$, there was a reversal of Q_M to values similar to those measured at 200 µmol photons m^{-2} s^{-1} (T2) after 1 h in recovery light ($P = 0.001$). Dark-adapted maximum quantum yield values (F_V/F_M) did not change from before to after the experiment, with initial F_V/F_M values of 0.544 ± 0.020 and 0.549 ± 0.008, and recovered F_V/F_M values of 0.562 ± 0.013 and 0.561 ± 0.017 in the control and light treated foraminifera ($n = 4$) respectively.The de-epoxidation ratio of the photoprotective xanthophyll pigments, increased to a maximum at 400 and 800 µmol photons m^{-2} s^{-1} ($P < 0.001$) and recovered to values measured at 200 µmol photons m^{-2} s^{-1} (T2) an hour after being returned to control light levels (130 µmol photons m^{-2} s^{-1}; Figure 1b),

following the same pattern as Q_M. The xanthophyll de-epoxidation ratio did not change in *M. vertebralis* under constant light.

Light stress results in symbiont retraction into the test

Symbiont retraction into the test was measured via changes in surface colour and reflectance. As the symbionts withdrew, more of the white test was exposed, causing an increase in the relative pixel intensity (whiteness) of the corresponding image or increasing spectral reflectance. The downward migration of symbionts, as measured by change in surface colour (Supplementary movie 1), resulted in a significant increase in pixel intensity (whitening due to exposure of the calcite test and loss of absorption by symbionts) with increased irradiance ($P = 0.002$; blue circles). There was no change in pixel intensity of the control foraminifera on either their exposed surface (black circles) or shaded underside (black triangles; Figure 1c). There was however, a decrease ($P = 0.002$) in pixel intensity (darkening) on the underside of the light treated foraminifera (blue triangles; Figure 1c), indicative of an increase in symbiont density on the shaded side. An increase ($P < 0.001$) in absolute reflectance (relative to a white Spectralon® standard) was detected with increased irradiance (Figure 1d), with the total integrated reflectance increasing from 30% in foraminifera under initial light conditions to 50% reflectance after exposure for 1 h at 800 µmol photons m^{-2} s^{-1} (Figure 1e; $P < 0.001$). The change in total reflectance was uniform across all wavelengths, where the major absorption bands of the chlorophyll *a*, c_2 and peridinin of the *Symbiodinium* changed equally with retraction into the test (Figure 1d and 1f), suggesting no change in relative composition or loss of pigments.

To confirm a vertical downward migration of symbionts through the interstitial channels of the foraminiferal skeletal structure and visualise the localisation of symbionts within the test, tissue sections were made of foraminifera taken from low (130 µmol photons m^{-2} s^{-1}), moderate (400 µmol photons m^{-2} s^{-1}), and high light (800 µmol photons m^{-2} s^{-1}) treatments (Figure 2). Histological

examination demonstrated that the symbionts relocated to the far side of the foraminiferal test when incoming irradiance was sufficiently high (Figure 2b). While the animal tissue fluoresced both in red and green, the stronger red auto-fluorescence of the algal chlorophyll resulted in a clear red colouration where symbionts were present in the tissue. After one hour under control light, the majority of the symbionts were close to the surface of the foraminifera (Figure 2b, left). At moderate irradiance (400 µmol photons m^{-2} s^{-1}), the symbionts were distributed throughout the test (Figure 2b, middle), while at the highest irradiance (800 µmol photons m^{-2} s^{-1}) the greatest symbiont density was seen in the under-most chambers of the foraminifera (Figure 2b, right).

Symbiont migration is host-mediated

The symbiont morphology was coccoid (Supplementary Figure S2), indicative of non-motile cells (Freudenthal, 1962). Cells incubated with a fluorescent membrane vacuole stain (Trautman et al, 2002) were highly fluorescent, showing the presence of a symbiosome encasing each cell (Supplementary Figure S2). To further investigate the host mechanism of symbiont relocation, we measured symbiont movement in the presence of the actin filament inhibitor cytochalasin B. The reduction in the photosynthetic efficiency ($\Delta F/F_M'$) of foraminifera exposed to high light, was greater in those treated with cytochalasin B (5 µg mL^{-1}; Figure 3a; $P = 0.001$), where the $\Delta F/F_M'$ at 800 µmol photons m^{-2} s^{-1} was zero (indicative of symbiont death) in 6 of the 8 specimens, highlighting the efficacy of symbiont retraction in providing photoprotection. The addition of cytochalisin B resulted in a 70% reduction in symbiont retraction at 800 µmol photons m^{-2} s^{-1} compared with the controls (Figure 3b; $P < 0.001$). Similarly, time lapse fluorescence microscopy of individual test chambers (Figure 4a) showed a significant decline in symbiont movement in the presence of the actin filament inhibitor (Supplementary movie 2), where the addition of 20 µg mL^{-1} resulted in a 90% reduction in movement (Figure 4b; $P < 0.001$). Importantly, cytochalasin B has been shown not to affect

movement in ciliates or flagellates at concentrations up to 50 µg mL^{-1} (Carter, 1967), more than twice the concentration employed in this study (5-20 µg mL^{-1}). As such, it is unlikely that the cytochalasin B would have inhibited any movement driven by *Symbiodinium*.

Symbiont photosynthetic activity drives stress signalling to the host

To explore whether the signal for symbiont retraction was directly related to photosynthetic stress, we sought to find changes in the symbiont response when photosynthesis was reduced. We used the photosynthetic inhibitor 3-(3,4-dichlorophenyl)-1,1-dimethylurea (DCMU) with the expectation that failure to remove the symbionts under high light would indicate communication between the symbiotic partners is photosynthetically-driven. In the DMSO control treatment, we measured a 73% reduction in photosynthetic efficiency at high light compared with the controls (Figure 5; $P < 0.001$), where effective quantum yield of PSII ($\Delta F/F_M'$) in the control was 0.45 at 130 µmol photons m^{-2} s^{-1} and dropped to around 0.12 at 800 µmol photons m^{-2} s^{-1}, equivalent to the $\Delta F/F_M'$ in the first set of experiments (Figure 1a). In contrast, in the presence of DCMU, $\Delta F/F_M'$ was 0.14 at control irradiances dropping below 0.05 at higher light (Figure 5), where 6 out of the 8 foraminifera had no variable fluorescence. We found that DCMU (10 µM), increased pixel intensity (symbiont retraction) by 20 and 27% in both the control (130 µmol photons m^{-2} s^{-1}) and high light (800 µmol photons m^{-2} s^{-1}) treatments, respectively (Figure 5; $P = 0.001$), showing there was an initial retraction (increased reflectance) of symbionts with the addition of DCMU. There was however, no additional retraction with exposure to high light resulting in a 58% reduction in pixel intensity compared with control incubations (Figure 5).

Discussion

277 Photoprotection is essential in shallow reef systems where irradiance often exceeds the capacity for
278 photosynthesis (Brown et al, 1999). Therefore, to avoid cellular damage or a breakdown in the
279 symbiosis, symbiotic partnerships are dependent on the ability of the symbiont and/or host to
280 regulate incoming irradiance. In the present study, the photophysiological responses of the symbionts
281 within *M. vertebralis* were consistent with general phototrophic responses to high light, with a
282 decline in photosynthetic efficiency and increase in energy dissipation, all indicative of light stress
283 (Müller et al., 2001). However, the rapid recovery in photosynthetic efficiency and concomitant
284 reversal of excitation pressure over PSII (Q_M) after return to low light, suggests that long-term
285 damage to the photosystem was largely avoided (Müller and Niyogi, 2001). In addition to increasing
286 photosynthetic stress, we also showed that the symbionts relocated from the surface to the middle or
287 underside of the foraminiferal test depending on the level of irradiance. These results demonstrate a
288 correlation between the level of photosynthetic stress (light intensity) and the level of retraction, and
289 thus protection. While *Symbiodinium* showed photosynthetic plasticity, it is evident that the physical
290 relocation of surface symbionts into the foraminiferal test contributed to preventing long-term
291 photosynthetic damage. This is supported by a previous study which found that only 30% of the
292 incoming irradiance was able to penetrate to the bottom of the test of *M. vertebralis* (Kohler-Rink
293 and Kühl, 2000). In addition to the inherent shading effect of the test itself (Kohler-Rink and Kühl,
294 2000), the increased reflectivity of the test decreased the incoming irradiance by an additional 20%
295 upon symbiont retraction. The efficacy of this photoprotective strategy is supported by the high
296 photosynthetic activity measured in symbionts on the underside of the test during exposure to high
297 irradiance and the rapid reversibility in photosynthetic quenching, Q_M and xanthophyll pigment
298 epoxidation of surface symbionts when incoming irradiance was lowered. Further support for the
299 effectiveness of the protection offered by the host is provided by the fluorescence measurements in
300 the presence of cytochalasin B, which showed that when vertical migration was prevented, the
301 photosynthetic activity of the symbionts exposed to high light was severely inhibited with no

variable fluorescence detectable in 6 of the 8 specimens. It cannot be ruled out, however, that this effect might also have been a result of some inhibitory effect of the cytochalasin B on the chloroplast repair system in the symbionts. The small yet significant increase in pixel intensity (whitening) observed at the highest light level in the presence of cytochalasin B, could in fact be attributed to loss of colouration from photobleaching of the chlorophyll in the immobilised symbionts. If so, this further supports the importance of this mechanism in the photoprotection of the symbionts in *M. vertebralis*.

The concept of phototaxis as a means for optimising light for photosynthesis in free-living microalgae is well studied. However, due to the inherent complexity of organisms living in symbioses, less is known about light regulation in symbiotic algae, and much less about the role of the host in this regulation. Until now, the only research on phototaxis in benthic endosymbiotic foraminifera has been focused on their propensity for seeking out shade through pseudopodal locomotion when exposed to high irradiances (Sinutok et al, 2013; Zmiri et al, 1974; Lee et al, 1980). In the only other study reporting the observation of intracellular phototaxis in *M. vertebralis,* the movement was believed to be driven by the symbionts themselves through flagella propulsion (Ross, 1972). However, the data presented here provides strong evidence for the phototaxic movement being host- rather than symbiont-driven: the coccoid, as opposed to gymnodinioid morphology of the symbionts is indicative of *Symbiodinium* in their non-motile, vegetative stage (Freudenthal, 1962), and the presence of a symbiosome membrane around the symbiont cells precludes the likelihood that symbionts could propel or move themselves within the host tissue. We saw a significant reduction in symbiont retraction and symbiont movement within individual chambers of the foraminifera test when actin filament contraction was inhibited (Estensen et al, 1971). This corroborates that the movement is host-mediated, as well as provides the first insight into the mechanisms behind this movement.

326 The ability to adjust intracellular symbiont position is likely an important means to optimise carbon
327 production, calcification and minimise photosynthetic damage, and can be described as akin to the
328 chloroplastic migration observed in phototrophic organisms, also known as chloroplast
329 photorelocation (Suetsugu and Wada, 2012). This light-dependent process optimises photosynthesis
330 and photo-protection through dispersion or aggregation of the chloroplasts to maximise light capture
331 or shading, respectively (Wada, 2013). The action of chloroplast photorelocation is driven by the
332 common motorproteins actin and myosin (Suetsugu and Wada, 2012), which together with
333 microtubules are responsible for the movement of cellular organelles in eukaryotic organisms. In the
334 case of photo-symbiotic organisms, however, the chloroplast is replaced by an entire algal cell. One
335 of few known examples of photo-relocation in a symbiotic organism is that of the single-celled
336 protist *Paramecium bursaria.* Known as the "green Paramecium", *P. bursaria* is symbiotic with the
337 green, non-motile microalgae *Chlorella*. When exposed to high light, *P. bursaria* will aggregate its
338 symbionts, presumably to shade both the host and the *Chlorella* cells, while it distributes the
339 *Chlorella* cells evenly in low light, maximising light uptake (Summerer et al, 2009). The phototaxis
340 shown here demonstrates photorelocation in *M. vertebralis* as a means of optimising light capture
341 and protection. The dynamic nature of the regulation of endosymbiont location by the host suggests
342 that it is closely coupled with the intensity of the incoming irradiance and the time of exposure.
343 Furthermore, the ability for *M. vertebralis* to move its symbionts within its test may explain its
344 propensity to attach to opaque surfaces (Sinutok et al, 2011; Sinutok et al, 2013), thereby eliminating
345 light input from the attached side and thus optimise the efficacy of shading and photoprotection
346 during the retraction of the symbionts.

347 The vertical migration away from high light, demonstrates a link between the symbiont stress and the
348 host's regulation of symbiont positioning, indicative of direct communication between the two
349 partners. In high light, the photosynthetic stress experienced by the symbiont is converted to a signal
350 that leads to reorganisation by the protist to ensure no damage to its energy-producing 'solar cells'.

351 This not only reduces the likelihood of photosynthetic damage from increased reactive oxygen, but
352 enables carbon-fixation and possibly light-dependent calcification, as observed in other foraminifera
353 (Hallock, 1981; Lea et al, 1995), to continue unimpeded. By chemically reducing the photosynthetic
354 efficiency of the symbionts (addition of DCMU), under control light conditions, partial retraction of
355 symbionts was observed, indicative of photosynthetic stress. However, the addition of high light
356 further quenched the photosystem to dysfunctional levels ($\Delta F/F_M' < 0.05$) but did not induce any
357 further vertical migration. The lack of movement under high light indicates a photosynthetically-
358 derived communication signal between partners, where the host's removal of its symbionts relies on
359 an info-chemical or signal that is generated by photosynthesis. Furthermore, as DCMU blocks the
360 transport of electrons through the photosynthetic electron transport chain at the beginning of the
361 photochemical pathway, it would suggest that any signalling molecule is a result of downstream
362 processes, relying on photosynthates (ATP, NADPH) derived from photosynthetic electron transport
363 and carbon fixation. One potential candidate signal molecule worthy of investigation could be a type
364 of reactive oxygen that is produced during photosynthetic stress (Lesser 2006).

365 This study has described negative phototaxis of symbionts in *M. vertebralis* in response to high light,
366 and confirmed that this movement is not flagellate driven. We uncovered a novel mechanism for
367 host-mediated photoprotection via the intracellular relocation of endosymbionts, whereby the host,
368 upon receiving a signal from the symbionts, mobilises cellular proteins to relocate the symbionts
369 deeper within its calcium carbonate test, thus providing protection and ensuring the health of the
370 partnership. Furthermore, the behavioural response described here suggest phototaxis is driven by
371 symbiont stress signalling, where the info-chemical is derived from downstream processes of the
372 photosynthetic electron transport chain. Our findings highlight the central importance of the host in
373 photo-symbiotic photoprotection. The dynamic nature of the photo-regulatory response described
374 here opens up new avenues to investigate symbiont-host stress physiology and symbiont-host
375 signalling for other photo-symbiotic species, such as corals, where the largest knowledge gap is the

communication or signalling between the host and the symbiont during physiological stress that results in coral bleaching, the catastrophic collapse of the symbiotic partnership.

Acknowledgements

We are grateful for the technical assistance of Jacqueline Loyola-Echeverria with the histological analysis and thank Dr Jean-Baptiste Raina for his helpful comments on the manuscript. We would also like to thank the staff at the Heron Island research station (HIRS). K.P. was supported by a UTS Chancellor's Postdoctoral Fellowship. *Marginopora vertebralis* were collected under the Great Barrier Reef Marine Parks permit G14/36977.1. issued to K.P. and D.A.N.. Author Contributions: K.P. and D.A.N. designed and performed research; P.J.R. contributed analytical tools; K.P. and D.A.N. analysed data; K.P. and D.A.N. wrote the paper.

The authors declare no conflict of interest.

Supplementary information is available at the end of this document.

394 **References**

395

396 Baker AC. (2003). Flexibility and specificity in coral-algal symbioses: diversity, ecology, and
397 biogeography of Symbiodinium. *Annu Rev Ecol Syst* 34:661-689.

398

399 Brown BE, Ambarsari I, Warner ME, Fitt WK, Dunne RP, Gibb SW. et al. (1999). Diurnal changes
400 in photochemical efficiency and xanthophyll concentrations in shallow water reef corals:
401 Evidence for photoinhibition and photoprotection. *Coral Reefs* 18:99-105.

402

403 Brown BE, Downs CA, Dunne RP, Gibb SW. (2002). Preliminary evidence for tissue retraction as a
404 factor in photoprotection of corals incapable of xanthophyll cycling. *J Exp Mar Biol Ecol*
405 277:129-144.

406

407 Carter SB. (1967). Effects of Cytochalasin on Mammalian Cells. *Nature* 213(5073):261-264.

408

409 Dimond JL, Holzman BJ and Bingham BL (2012) Thicker host tissues moderate light stress in a
410 cnidarian endosymbiont. *J Exp Biol* 215:2247-2254.

411

412 Doo SS, Hamylton S, Byrne M. (2012). Reef-Scale Assessment of Intertidal Large Benthic
413 Foraminifera Populations on One Tree Island, Great Barrier Reef and Their Future Carbonate
414 Production Potential in a Warming Ocean. *Zool Stud* 51:1298-1307.

415

416 Dove SG, Lovell C, Fine M, Deckenback J, Hoegh-Guldberg O, Iglesias-Prieto R, et al. (2008).
417 Host pigments: potential facilitators of photosynthesis in coral symbioses. *Plant Cell Environ*
418 31:1523-1533.

Estensen RD, Rosenberg M, Sheridan JD. (1971). Cytochalasin B: microfilaments and contractile processes. *Science* 173:356-358.

Freudenthal HD. (1962). Symbiodinium Gen Nov and Symbiodinium Microadriaticum sp Nov, a Zooxanthella - Taxonomy, Life Cycle, and Morphology. *J Protozool* 9:45-52.

Hallock P. (1981). Light dependence in Amphistegina. *J Foraminif Res* 11:40-46.

Iglesias-Prieto R, Beltrán VH, LaJeunesse TC, Reyes-Bonilla H, Thomé PE. (2004). Different algal symbionts explain the vertical distribution of dominant reef corals in the eastern Pacific. Proc. R. Soc. Lond. B 271: 1757-1763.

Iglesias-Prieto R, Trench RK. (1994). Acclimation and adaptation to irradiance in symbiotic dinoflagellates. I. Responses of the photosynthetic unit to changes in photon flux-density. *Mar Ecol Prog Ser* 113:163-175.

Iglesias-Prieto R, Trench RK. (1997). Acclimation and adaptation to irradiance in symbiotic dinoflagellates. II. Response of chlorophyll-protein complexes to different photon-flux densities. *Mar Biol* 130:23-33.

Jones RJ, Hoegh-Guldberg O. (2001). Diurnal changes in photochemical efficiency of the symbiotic dinoflagellates (Dinophyceae) of corals: photoprotection, photoinactivation and the relationship to coral bleaching. *Plant Cell Environ* 24:89-99.

444 Khare N, Nigam R. (2000). Laboratory experiment to record rate of movement of cultured benthic
445 foraminifera. *ONGC Bull* 37:53-61.
446
447 Kohler-Rink S, Kühl M. (2000). Microsensor Studies of photosynthesis and respiration in larger
448 symbiotic foraminifera. I. The physico-chemical microenvironment of *Marginopora vertebralis*,
449 *Amphistegina lobifera* and *Amphisorus hemprichii*. *Mar Biol* 137:473-486.
450
451 Langer MR, Silk MT, Lipps JH. (1997). Global ocean carbonate and carbon dioxide production; the
452 role of reef foraminifera. *J Foraminif Res* 27:271-277.
453
454 Lea DW, Martin PA, Chan DA, Spero HJ. (1995). Calcium Uptake and Calcification Rate in the
455 Planktonic Foraminefera Orbulina Universa. *J Foraminif Res* 25:14-23.
456
457 Lee JJ, McEnery ME, Garrison JR. (1980). Experimental studies of larger foraminifera and their
458 symbionts from the Gulf of Eilat on the Red Sea. *J Foraminif Res* 10:31-47.
459
460 Lee JJ. (2006). Algal symbiosis in larger foraminifera. *Symbiosis* 42:63-75.
461
462 Lesser MP. (2006). Oxidative stress in marine environments: biochemistry and physiological
463 ecology. *Annu Rev Physiol* 68:253-278.
464
465 Müller P, Li X-P, Niyogi KK. (2001). Non-photochemical quenching. A response to excess light
466 energy. *Plant Physiol* 125:1558-1566.
467

468 Pawlowski J, Holzmann M, Fahrni JF, Pochon X, Lee JJ. (2001). Molecular identification of algal
469 endosymbionts in large miliolid foraminifera: 2. Dinoflagellates. *J Euk Microbiol* 48:368-373.
470
471 Ross CA. (1972). Biology and Ecology of Marginopora-Vertebralis (Foraminiferida), Great Barrier
472 Reef. *J Protozool* 19:181-192.
473
474 Salih A, Larkum ADW, Cox G, Kühl M, Hoegh-Guldberg O. (2000). Fluorescent pigments in corals
475 are photoprotective. *Nature* 408:850-853.
476
477 Schneider CA, Rasband WS, Eliceiri KW. (2012). NIH Image to ImageJ: 25 years of image analysis.
478 *Nature Methods* 9:671-675.
479
480 Schreiber U. (2004). Pulse-amplitude-modulated (PAM) fluorometry and saturation pulse method.
481 In: Papagiorgiou GG (ed) Advances in photosynthesis and respiration, vol 19. Springer,
482 Dordrecht, pp 279–319.
483 Sinutok S, Hill R, Doblin MA, Wuhrer R, Ralph PJ. (2011). Warmer more acidic conditions cause
484 decreased productivity and calcification in subtropical coral reef sediment-dwelling calcifiers.
485 *Limnol Oceanogr* 56:1200-1212.
486
487 Sinutok S, Hill R, Doblin MA, Ralph PJ. (2013). Diurnal photosynthetic response of the motile
488 symbiotic benthic foraminiferan *Marginopora vertebralis*. *Mar Ecol Prog Ser* 478:127-138.
489
490 Suetsugu N, Wada M. (2012). Chloroplast Photorelocation Movement: A Sophisticated Strategy for
491 Chloroplasts to Perform Efficient Photosynthesis. In: Najafpour, MM (ed). *Advances in*
492 *Photosynthesis - Fundamental Aspects*. InTech, pp. 215-234.

Summerer M, Sonntag B, Hörtnagl P, Sommaruga R. (2009). Symbiotic Ciliates Receive Protection Against UV Damage from their Algae: A Test with Paramecium bursaria and Chlorella. *Protist* 160:233-243.

Trautman DA, Hinde R, Cole L, Grant A, Quinnell R. (2002). Visualisation of the symbiosome membrane surrounding cnidarian algal cells. *Symbiosis* 32:133-145.

van Heukelem L, Thomas C. (2001). Computer-assisted high-performance liquid chromatography method development with applications to the isolation and analysis of phytoplankton pigments. J Chromatogr A 910:31–49

Wada M. (2013). Chloroplast movement. *Plant Sci* 210:177-182.

Wangpraseurt D, Larkum AWD, Franklin J, Szabo M, Ralph PJ, Kühl M. (2014). Lateral light transfer ensures efficient resource distribution in symbiont-bearing corals. *J Exp Biol* 217:489-498.

Zmiri A, Kahan D, Hochstein S, Reiss Z. (1974). Phototaxis and thermotaxis in some species of *Amphistegine* (Foraminifera). *J Protozool* 21:133-138.

514 **Figure legends**

515 **Figure 1 | Change in photophysiology and reflectance under different irradiance treatments**
516 **over time**. (a) Effective quantum yield of PSII ($\Delta F/F_M'$) for the surface (circles) and underside
517 (triangles) of *M. vertebralis* exposed to constant light (*CL*; black) and increasing light (*IL*; blue) over
518 3 h with a final hour of recovery (n = 8). (b) Excitation pressure over PSII (Q_M) on the surface of *M.*
519 *vertebralis* (circles; n = 8) and the de-epoxidation ratio of photoprotective pigments (bars; n = 3),
520 exposed to constant low (130 µmol photons m^{-2} s^{-1}) light (black) and increasing irradiance over 3 h +
521 recovery (blue). (c) Relative change in average pixel intensity on the surface (circles) and underside
522 (triangles) of *M. vertebralis* exposed to constant (black) and increasing light over 3 h + recovery
523 (blue) (n = 5-8). (d) Spectral reflectance as a percentage of a pure white standard measured on the
524 surface of *M. vertebralis* exposed to increasing irradiances. Arrows indicate characteristic absorption
525 wavelengths of *Symbiodinium*: chlorophyll *a* (435-440, 675 nm), chlorophyll *c* (460 nm) and
526 peridinin (480-490 nm), dashed lines indicate SEM (n = 8). (e) Total integrated reflectance at the
527 surface of *M. vertebralis* exposed to increasing irradiances over time (T0-T3) (n = 8). (f)
528 Photographs illustrating the sequential whitening (from top left to bottom right) of one *M. vertebralis*
529 exposed to high light. Scale bar = 5 mm. Data represent mean ± SEM. Asterisk (*) indicates values
530 that are significantly different between light treatments and superscript letters denote significantly
531 different over time ($p < 0.05$).

532

533 **Figure 2 | Tissue sections illustrating the localisation of the symbionts within the test of *M.***
534 ***vertebralis* exposed to 130, 400 and 800 µmol photons m^{-2} s^{-1}.** (a) Complete tissue section of an *M.*
535 *vertebralis* tests, scale bar = 200 µm (b) close up of three different tissue sections from foraminifera
536 exposed to different light intensities (indicated in the picture), scale bar = 50 µm. Green is the auto-
537 fluorescence of the animal tissue and red is the symbiont chlorophyll.

538

539 **Figure 3 | Change in photoshynthetic efficiency and pixel intensity in the presence of the actin**
540 **inhibitor Cytochalasin B.** (a) Effective quantum yield of PSII ($\Delta F/F_M'$) at constant (*CL*; black) and
541 increasing (*IL*; blue) light intensities, in the presence (Cyto; circles) and absence (DMSO; triangles)
542 of cytochalasin B. Insert shows the $\Delta F/F_M'$ at 800 µmol photons m^{-2} s^{-1} as a percentage of the initial
543 values. (b) Relative change in pixel intensity at constant (black) and increasing light (blue)
544 intensities, in the presence (circles) and absence (triangles) of cytochalasin B. Data represent mean ±
545 SEM, n = 6-8. Asterisk (*) indicates values that are significantly different between light treatments
546 and superscript letters denote significantly different over time ($p < 0.05$).

547

548 **Figure 4 | Change in symbiont motility in the presence of cytochalasin B.** (a) S*ymbiodinium* (red)
549 within individual chambers of *M. vertebralis* test (green) (b) average speed of movement of
550 S*ymbiodinium* within chambers incubated with 0, 10 and 20 µg mL^{-1} of cytochalasin B, respectively,
551 as a percent of control (data were square root transformed; n = 18). Scale bar = 25 µm. Data
552 represent mean ± SEM. Superscript letters denote significant difference between treatments ($p <$
553 0.05).

554

555 **Figure 5 | Symbiont photosynthesis and vertical migration in the presence of DCMU.** Relative
556 change in pixel intensity (bars) and effective quantum yield of PSII (diamonds) in *M. vertebralis*
557 exposed to 130 µmol photons m^{-2} s^{-1} (black bars) and 800 µmol photons m^{-2} s^{-1} (blue bars) in the
558 presence of DMSO (control) or DCMU (n = 6-8). Error bars on $\Delta F/F_M'$ are smaller than the symbol.
559 Data represent the mean ± SEM. Superscript letters denote significant difference between treatments
560 ($p < 0.05$).

561

562 Figure 1.

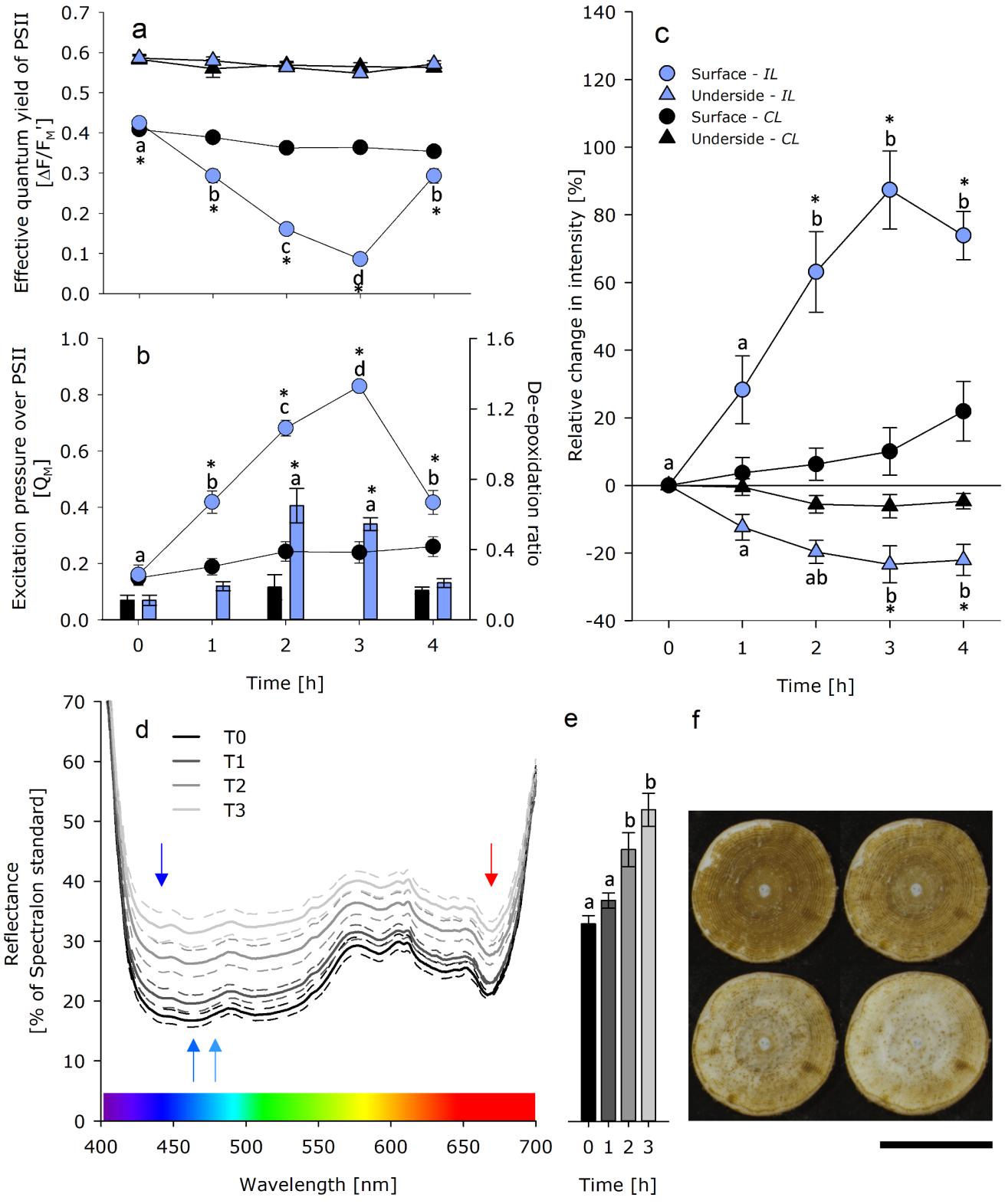

563

564

565 Figure 2.

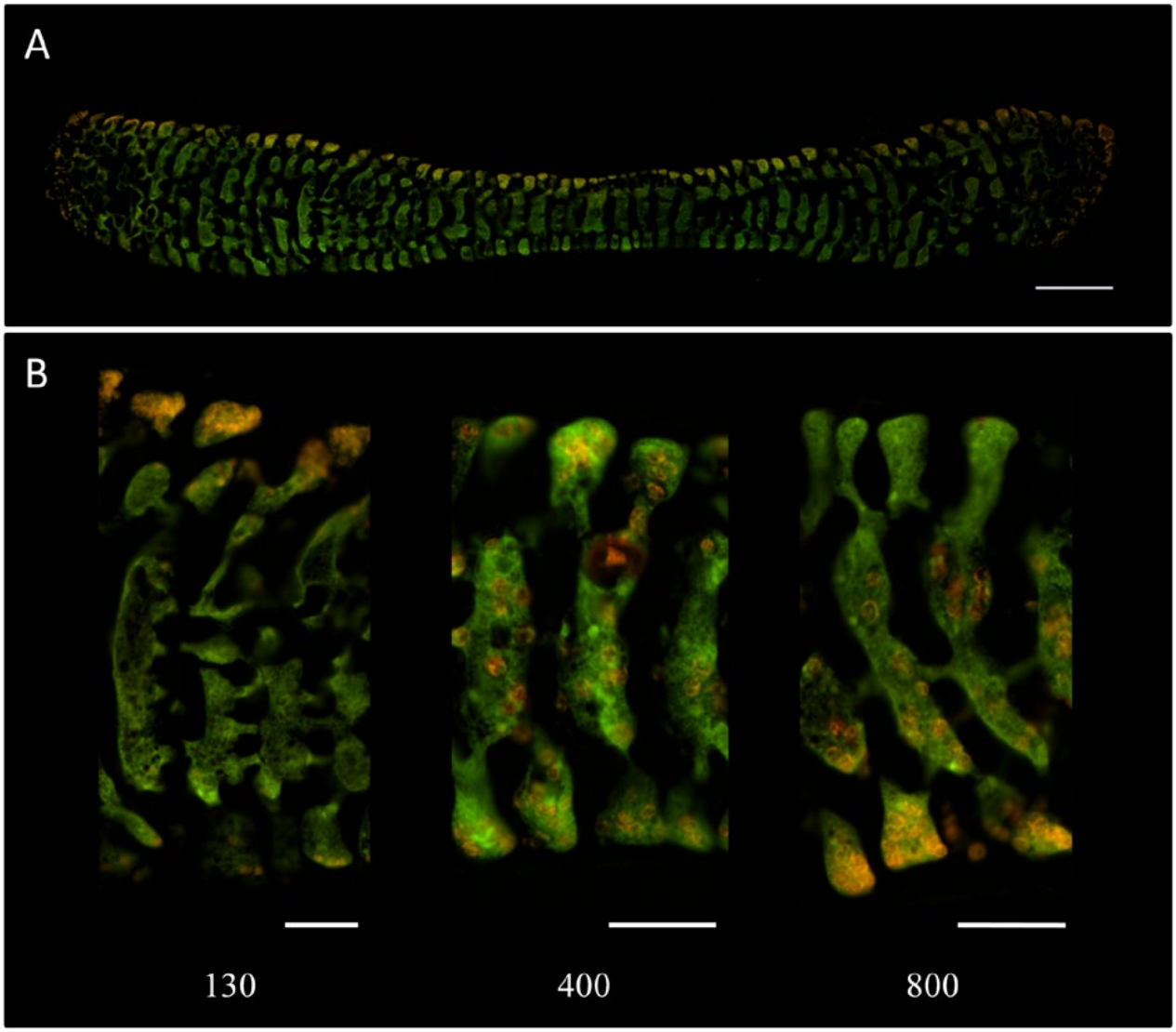

566

567

568 Figure 3.

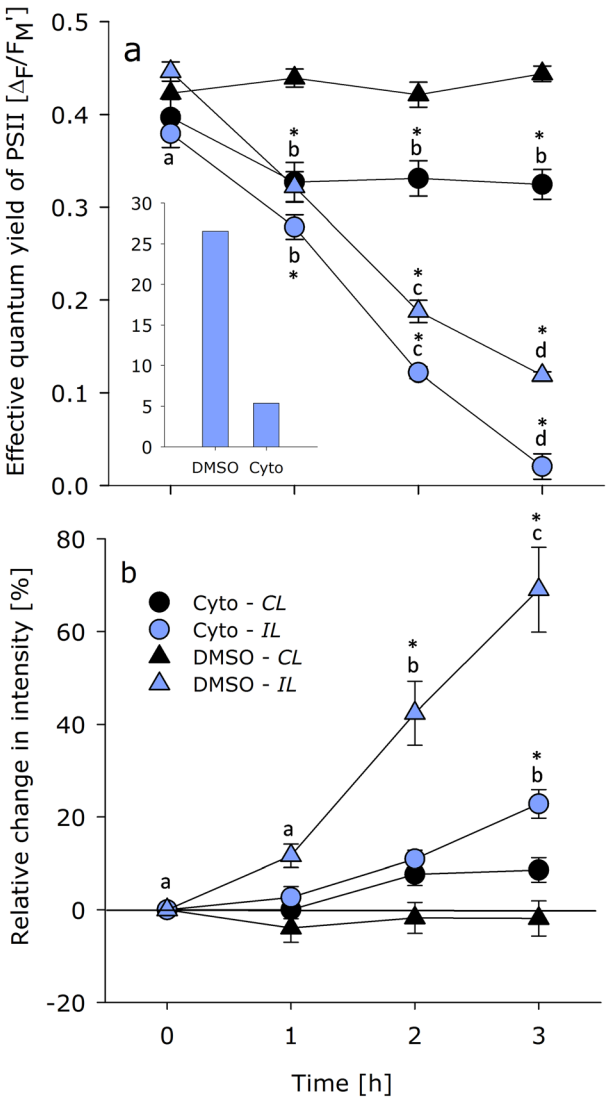

569

570

571 Figure 4.

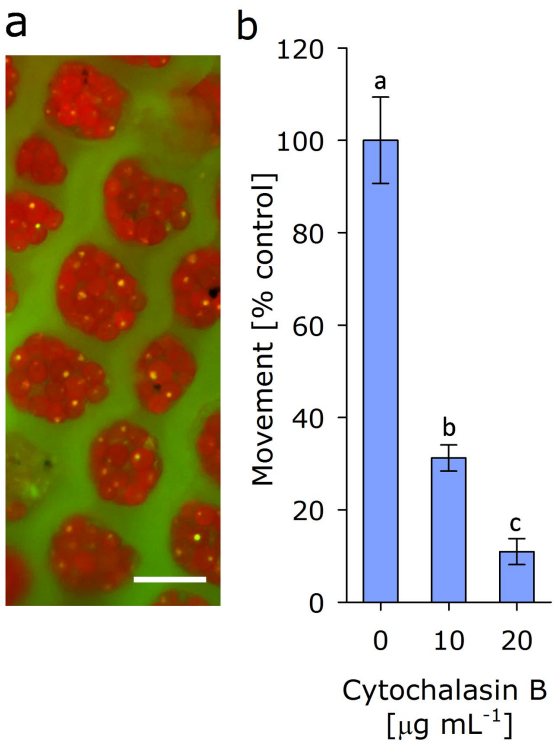

572

573

574 Figure 5.

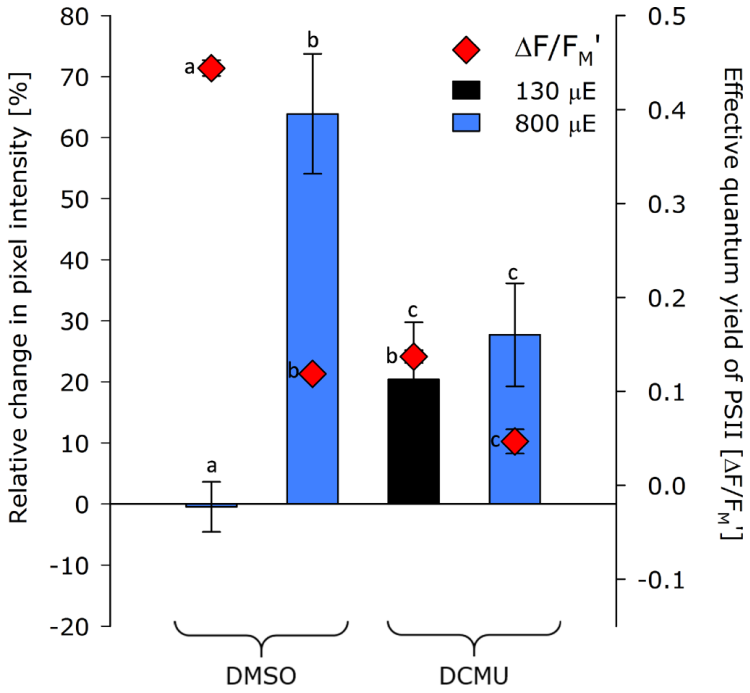

575

576

Supplementary information

Method description for supplemental movies 1 and 2.

To view movies please go to the respective Supplementary Information page on the ISME Journal website.

Time-lapse of symbiont retraction into *M. vertebralis* test: Symbiont retraction was imaged using a fluorescence dissection microscope. The foraminifera was positioned in a black bottom glass beaker containing seawater at ambient temperature. In order to induce light stress and symbiont retraction, high intensity light was supplied from above using microscope stereo lights. The foraminifera was imaged at approximately 30X every minute for one hour and images were combined into a video at a frame rate of 5 frames s^{-1}, equal to 300X real speed using the image software package ImageJ (see Supplemental Movie 1).

Video of symbiont movement in *M. vertebralis* test with and without Cytochalasin B: The movement of the symbionts within test chambers in the presence and absence of Cytochalasin B were captured using an inverted fluorescence microscope (Nikon *Ti*-eclipse). Prior to imaging, specimens were incubated in 1 mL of seawater with 0 or 20 µg mL^{-1} Cytochalasin B for 1 hour. The foraminifera were then positioned on a microscope slide in a drop of incubation water, and covered with a coverslip and spacer. Chambers of the foraminifera were imaged at 400X magnification in two fluorescent channels (Green – FITC, red – TexasRed), exploiting the auto-fluorescence of the skeleton and symbionts, respectively. An image was taken every minute over a period of 10 minutes in between which the foraminifera was left in the dark. Images from the two treatments were stitched and combined into a video at a frame rate of 5 frames s^{-1}, equal to 300X real speed, using the image software package ImageJ (see Supplemental Movie 2).

600 **Steady state light curve:** Following dark-adaptation (20 min), a steady state light curve was
601 performed on foraminifera using a Pulse Amplitude Modulated (PAM) fluorometer (Imaging PAM,
602 Max/K, Walz GmbH, Effeltrich, Germany), applying a high intensity pulse of light to saturate the
603 photosystem (saturating pulse width = 0.8 s; saturating pulse intensity > 3000 µmol photons m^{-2} s^{-1}).
604 Ten incrementing light levels (22, 32, 49, 76, 113, 156, 200, 314, 400, 800 µmol photons m^{-2} s^{-1})
605 were applied for 5 min each before recording the light-adapted minimum (F_T) and maximum
606 fluorescence (F_M') values. The relative electron transport rates (rETR) were calculated as ((F_M'-
607 F_T)/F_M')*PAR and photosynthetic parameters determined from a double exponential function fitted
608 to the data (Ralph and Gademann 2005).

609

610 **Symbiosome detection**: *M. vertebralis* were de-calcified in 0.5 M EDTA overnight. De-calcified
611 tests were then mashed up using a glass micro-pestle in 0.22 µm FSW and split into two samples,
612 one with the addition of the yeast vacuole membrane marker MDY-64 (10 µM; Life Technologies).
613 Following incubation (5 min) sample was centrifuged (4300g x 2 min), the supernatant removed and
614 resuspended in FSW. The sample was re-centrifuged (4300g x 2 min), supernatant removed and
615 pellet re-suspended in 100 µl of FSW. *Symbiodinium* were imaged using an inverted fluorescence
616 microscope (Eclipse-T*i*, Nikon Corporation, Japan) and 400X magnification and data collected using
617 NIS-Elements software (Nikon). All settings for fluorescence imaging were kept constant between
618 the control and MDY-64 incubated samples to avoid any bias from exposure time adjustments.
619 Standard excitation/emission filter sets were used for imaging: FITC (ex/em 500-540 nm) to
620 visualise the symbiosome and Texas Red (ex 532-587 nm/em 595 nm) to image auto-fluorescence of
621 the chlorophyll in the algal symbionts. Fluorescence images were analysed with the open source
622 image analysis software package ImageJ[35].

623

Figure S1

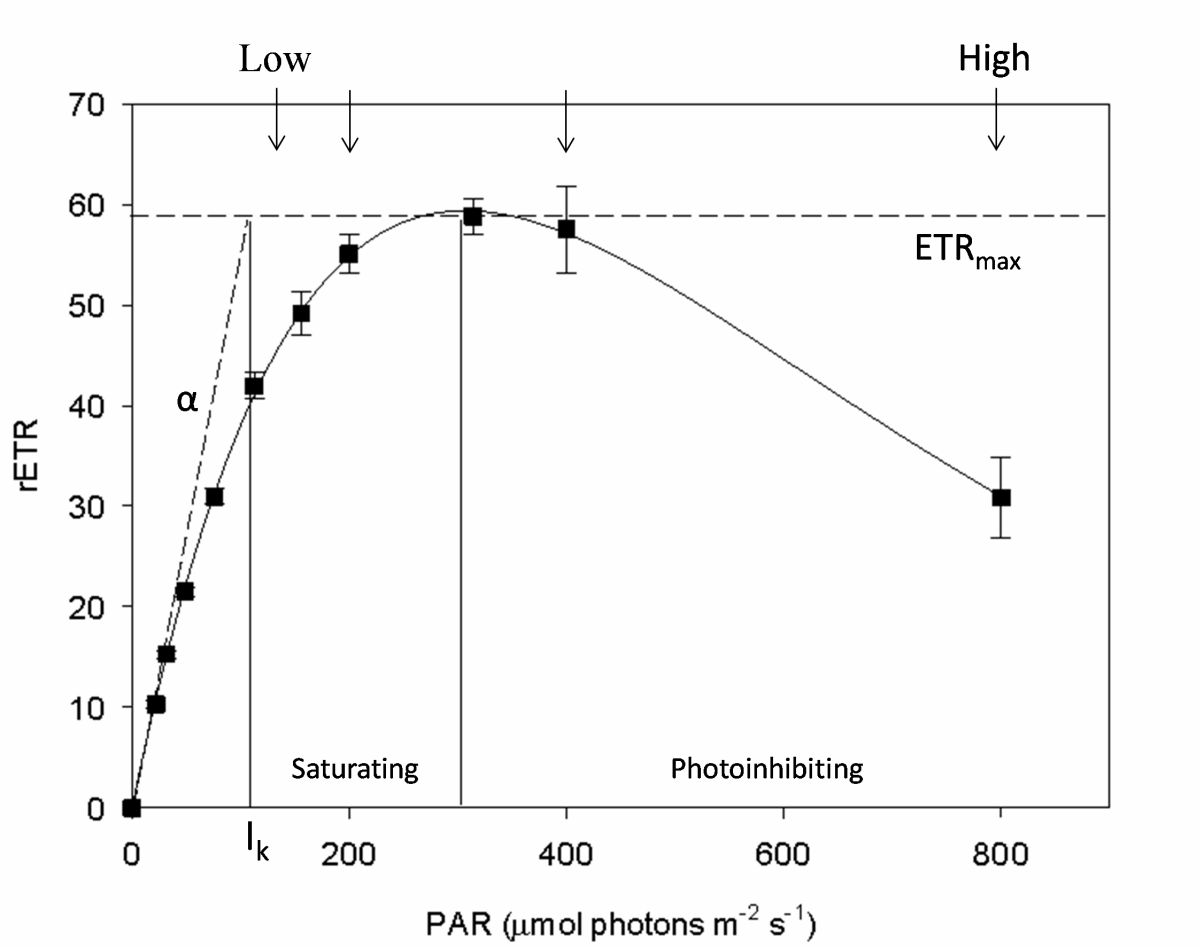

Figure S1 | Steady state light curves of *Marginopora vertebralis*. Relative electron transport rates (rETR) of Symbiodinium exposed to increasing light levels (5 min intervals). Minimum saturating irradiance (I_k). Dotted lines show maximum electron rate (ETR_{max}) and light utilization efficiency (α). Parameters derived from double exponential function according to Ralph and Gademann (2005). Down arrows indicate light levels used in the study. Data represent mean ± Standard Error (n=6).

Figure S2

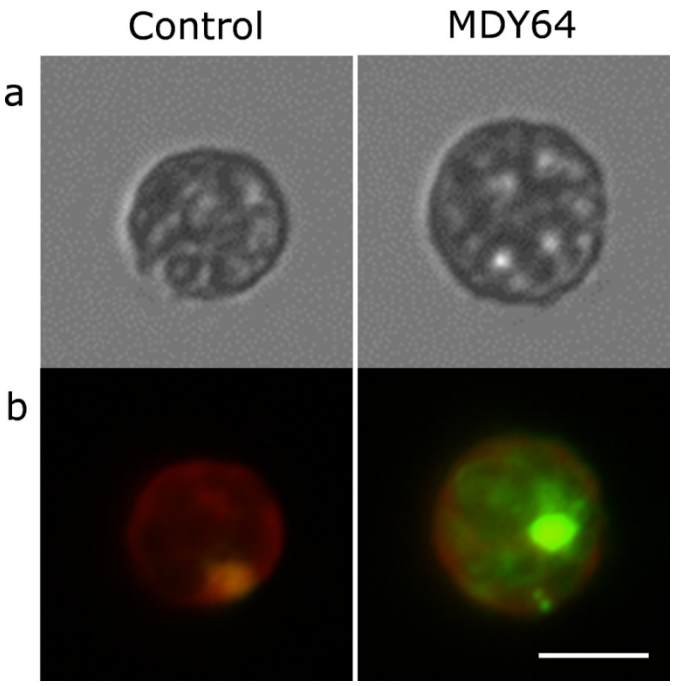

Figure S2 | Detection of symbiosome membrane around *Symbiodinium* isolated from *M. vertebralis*. Microscopy images (400x) of *Symbiodinium* cells isolated from foraminifera test illustrating coccoid (non-motile) morphology. Non-stained (left) and stained with the symbiosome dye MDY-64 (right). Red = chlorophyll autofluorescence (exposure time 300 ms) and Green = emission from MDY-64 (exposure time 210 ms). Scale bar = 5 µm.

References

Ralph PJ, Gademann R (2005). Rapid light curves: a powerful tool to assess photosynthetic activity. Aquat Bot 82:222-237.